Cancer Cell
Article

Significance of CD90$^+$ Cancer Stem Cells in Human Liver Cancer

Zhen Fan Yang,[1,2,*] David W. Ho,[1,2] Michael N. Ng,[1,2] Chi Keung Lau,[1,2] Wan Ching Yu,[1] Patricia Ngai,[1] Patrick W.K. Chu,[1] Chi Tat Lam,[1] Ronnie T.P. Poon,[1] and Sheung Tat Fan[1,*]
[1]Center for Cancer Research and Department of Surgery, The University of Hong Kong, Pokfulam, Hong Kong, China
[2]These authors contributed equally to this work.
*Correspondence: zfyang@hkucc.hku.hk (Z.F.Y.), stfan@hku.hk (S.T.F.)
DOI 10.1016/j.ccr.2008.01.013

SUMMARY

This study characterized cancer stem cells (CSCs) in hepatocellular carcinoma (HCC) cell lines, tumor specimens, and blood samples. The CD90$^+$ cells, but not the CD90$^-$ cells, from HCC cell lines displayed tumorigenic capacity. All the tumor specimens and 91.6% of blood samples from liver cancer patients bore the CD45$^-$CD90$^+$ population, which could generate tumor nodules in immunodeficient mice. The CD90$^+$CD44$^+$ cells demonstrated a more aggressive phenotype than the CD90$^+$CD44$^-$ counterpart and formed metastatic lesions in the lung of immunodeficient mice. CD44 blockade prevented the formation of local and metastatic tumor nodules by the CD90$^+$ cells. Differential gene expression profiles were identified in the CD45$^-$CD90$^+$ and CD45$^-$CD90$^-$ cells isolated from tissue and blood samples from liver cancer patients and controls.

INTRODUCTION

Cancer stem cells (CSCs) are the source of many solid tumor types (Al-Hajj et al., 2003; Singh et al., 2004; Collins et al., 2005; O'Brien et al., 2007; Ricci-Vitiani et al., 2007; Li et al., 2007), including hepatocellular carcinoma (HCC). HCC is the fifth most common cancer in the world and comprises more than 90% of human liver cancers. The incidence of HCC is increasing due to increased rates of hepatitis B and C viral infection (Llovet et al., 2003; McMahon, 2005; El-Serag, 2004). Hepatic resection and liver transplantation are the two main treatment modalities for HCC, and the 5 year survival rate correlates with tumor staging at the time of diagnosis (Mazzaferro et al., 1996; Llovet et al., 1999; Arii et al., 2000). The majority of HCC patients present with an advanced stage of cancer for which chemotherapy and radiotherapy have limited efficacy (Groupe d'Etude et de Traitement du Carcinome Hépatocellulaire, 1995; Lo et al., 2002). Hence, understanding the mechanism underlying hepatocarcinogenesis is essential for the management of liver malignancy.

CSCs have been characterized in solid tumors using a variety of stem cell markers, including CD133 (Tang et al., 2007). Although CD133 can identify CSCs in cell line-induced HCC (Suetsugu et al., 2006; Yin et al., 2007; Ma et al., 2007), the CD133$^+$ cells isolated from human tumor specimens are not well characterized. Furthermore, the CD133$^-$ cells also have the capacity to generate tumor nodules in immunodeficient mice, although at a higher cell number (Ma et al., 2007). Previously, we showed that CD133 is a marker of circulating endothelial progenitor cells (EPCs) in HCC patients (Ho et al., 2006). Together, the above evidence suggests that CD133 is not sufficiently sensitive or specific to be a marker of CSCs in liver malignancy.

CD90 (Thy-1) is a 25-37 kDa glycosylphosphatidylinositol (GPI)-anchored glycoprotein expressed mainly in leukocytes and is involved in cell-cell and cell-matrix interactions (Rege and Hagood, 2006). CD90 is also expressed by bone marrow-derived mesenchymal stem cells (Dennis et al., 2007) and hepatic stem/progenitor cells (HSPCs) (Lázaro et al., 2003; Herrera et al., 2006; Dan et al., 2006). In addition, CD90 expression was identified in murine breast CSCs (Cho et al., 2007) and primarily cultured CD133$^+$ glioblastoma CSCs (Liu et al., 2006). Based on the above findings, CD90 was used in the present study to identify potential hepatic CSCs from

SIGNIFICANCE

This study reveals that CD90 is a potential marker of liver CSCs, and the concomitantly expressed CD44 modulates the biological activity of the CD90$^+$ CSCs. The presence of local and circulating CSCs implies the aggressive phenotype of liver malignancy, in which the CD90$^+$CD44$^+$ cells contribute prominently to its aggressiveness and metastasis. The prevention of local and systemic tumor formation by CD44 blockade highlights the potential of CD44 as a therapeutic target for CD90$^+$ CSCs. The differential gene expression profiles of CSCs and normal stem cells suggest the importance of these genes in hepatocarcinogenesis. The identification of local and circulating CSCs provides a cellular basis of liver cancer development, recurrence, and metastasis and will favor the design of future therapeutic strategies.

Table 1. Comparison of Tumorigenic Capacity of the CD90$^+$ Cells from Different HCC Cell Lines

Cell Lines	% of CD90$^+$ Cells (in Total Cells)	Tumorigenicity (Cell No.)	Tumorigenicity (Time)	Metastasis	No. of Injected CD90$^+$ Cells	No. of Mice with Tumor Formation/ Total No. of Mice With Cell Injection		
						2 Months	3 Months	4 Months
MIHA	0	ND	ND					
HepG2	0.04 ± 0.01	1×10^7	3 months	no	5×10^2	0/3	0/3	0/3
					1×10^3	0/3	0/3	1/3
					5×10^3	0/3	1/3	0/2
					1×10^4	1/3	1/2	1/1
Hep3B	0.45 ± 0.06	1×10^6	2 months	no	5×10^2	0/3	0/3	0/3
					1×10^3	0/3	1/3	1/2
					5×10^3	1/3	1/2	1/1
					1×10^4	2/3	1/1	
PLC	0.48 ± 0.06	1×10^6	1 month	no	5×10^2	0/5	0/5	0/5
					1×10^3	1/5	2/4	1/2
					5×10^3	4/5	1/1	
					1×10^4	4/5		
Huh7	0.61 ± 0.18	1×10^6	1 month	no	5×10^2	0/3	0/3	0/3
					1×10^3	1/3	2/2	
					5×10^3	2/3	1/1	
					1×10^4	3/3		
MHCC97L	2.15 ± 0.14	2×10^5	3 weeks	yes	5×10^2	0/6	1/6	1/5
					1×10^3	3/5	2/2	
					5×10^3	5/5		
					1×10^4	5/5		
MHCC97H	2.34 ± 0.3	1×10^5	2 weeks	yes	5×10^2	0/3	1/3	1/2
					1×10^3	2/3	1/1	
					5×10^3	3/3		
					1×10^4	3/3		

MIHA is an immortalized nontumorigenic normal human hepatocyte cell line. ND, not determined. The number of the CD90$^+$ cells was expressed as mean percentage ± SD (representative of three independent experiments). Tumorigenicity by cell number was defined as the lowest number of total tumor cells that were capable of inducing tumor formation at 2 months after cell injection, whereas tumorigenicity by time was defined as the shortest time interval that was required for 1×10^6 total tumor cells to develop tumors. The sorted CD90$^+$ and CD90$^-$ cells from different cell lines were injected subcutaneously into two different sites of a same nude mouse. Animals were sacrificed when tumor nodules were identified in nude mice, otherwise the mice were monitored continuously until the second or third time point.

HCC cell lines, tumor specimens, and blood samples of liver cancer patients.

RESULTS

Tumorigenic Capacity of CD90$^+$ Cells Isolated from HCC Cell Lines

Six human HCC cell lines, specifically HepG2, Hep3B, PLC, Huh7, MHCC97L, and MHCC97H, and one immortalized nontumorigenic normal human hepatocyte cell line, MIHA (Pang et al., 2006), were used to screen for the expression of stem cell markers by flow cytometry. The tumorigenic potential of the 6 HCC cell lines ranges from low in HepG2 to high in MHCC97H. In the present study, tumorigenicity is defined as the capacity of a certain cell number, following serial dilution, to form tumor nodules in immunodeficient mice within a certain time interval (Table 1). Three time points were used for the assessment of tumorigenicity of cell lines and the cells isolated from human tumor specimens and blood samples. Differentially expressed stem cell markers were detected in the HCC cell lines, among which only the expression of CD90 correlated positively with tumorigenicity and metastatic properties of cell lines (see Table S1 available with this article online).

The CD90$^+$ cells were isolated from HCC cell lines using magnetic microbeads and injected subcutaneously into BALB/c nude mice using the CD90$^-$ cells as a control. Tumor nodules from the CD90$^+$ cells isolated from both MHCC97L and MHCC97H cell lines appeared after 3 months from 500 inoculated cells. When the cell number was increased to 1,000, the CD90$^+$ cells from 4 out of 6 HCC cell lines (PLC, Huh7, MHCC97L, and MHCC97H) generated tumor nodules in nude mice at 2 months. In cell line with low tumorigenic capacity, HepG2, a higher number of CD90$^+$ cells (5,000 cells at 3 months) or a longer observation time (4 months with 1,000 cells) was needed for tumor development (Table 1). In contrast, the CD90$^-$ cells from all cell lines tested did not induce tumor formation in nude mice, even 4 months after injecting 1×10^4 cells. MHCC97L cell line was chosen to illustrate histological characteristics of tumor xenografts

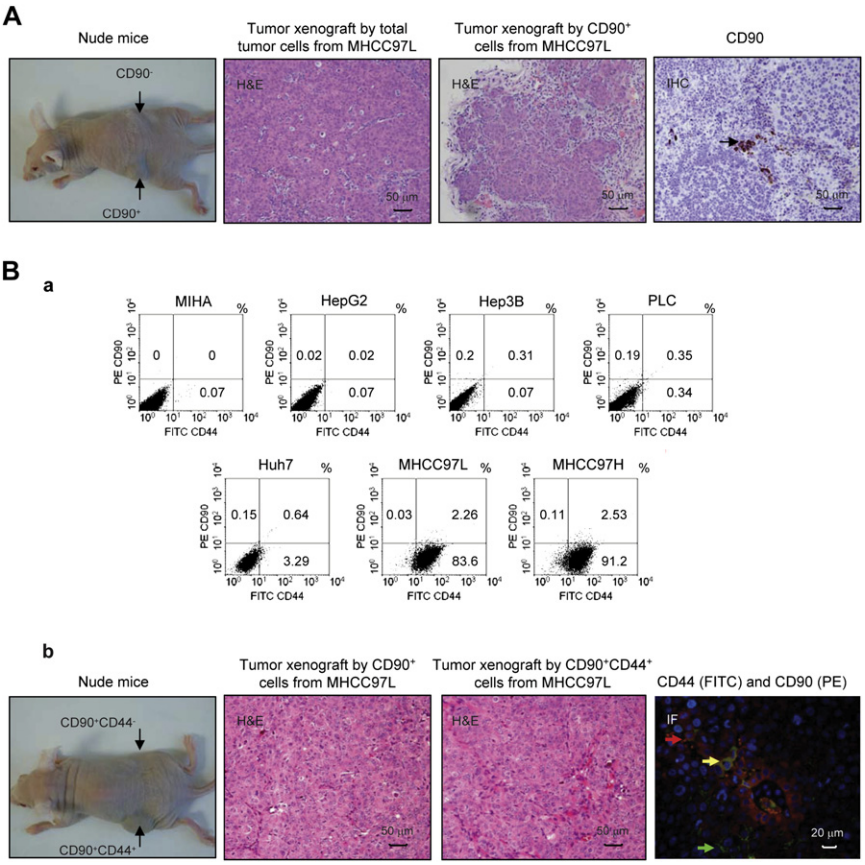

Figure 1. Tumorigenic Capacity of the CD90$^+$ or CD90$^+$CD44$^+$ Cells from MHCC97L Cell Line

(A) The CD90$^+$ and CD90$^-$ cells were isolated from MHCC97L cell line with a purity ranging from 80.1% to 83.2%, and each cell type was injected subcutaneously into two different sites of a same BALB/c nude mouse. After 2 months, the CD90$^+$ cells (cell number = 1 × 10^4), but not the CD90$^-$ cells, formed tumor nodules. Arrows indicate the site of CD90$^-$ or CD90$^+$ cell injection. Similar histological features were detected by hematoxylin-eosin (H&E) staining in tumor xenografts generated by total tumor cells (1 × 10^6) and the isolated CD90$^+$ cells (1 × 10^4). Immunohistochemical staining (IHC) identifies scattered and clustered distribution of the CD90$^+$ cells in tumor xenograft. An arrow points to a cluster of CD90$^+$ cells.

(Ba) Flow cytometry was used to conduct multi-marker analyses. No CD90$^+$CD44$^+$ cells were detected in MIHA cell line. In contrast, the CD90$^+$CD44$^+$ cells were detected in all HCC cell lines tested (HepG2, 0.02%; Hep3B, 0.31%; PLC, 0.35%; Huh7, 0.64%; MHCC97L, 2.26%; MHCC97H, 2.53%).

(Bb) The photo shows a tumor nodule at the site of injected CD90$^+$CD44$^+$ cells, but not at the site of injected CD90$^+$CD44$^-$ cells. The histological features of tumor xenograft induced by the CD90$^+$CD44$^+$ cells are comparable to that induced by the CD90$^+$ cells. Immunofluorescent staining (IF) reveals the presence of CD90 and CD44 double-positive cells in the generated tumor xenograft. Red, green, and yellow arrows point to the CD90$^+$, CD44$^+$, and CD90$^+$CD44$^+$ cells, respectively.

induced by total tumor cells (1 × 10^6) and the isolated CD90$^+$ cells (1 × 10^4). Hematoxylin-eosin (H&E) staining identified similar histological features in tumor xenografts generated by the above two types of cells. Immunohistochemical staining (IHC) analysis showed scattered and clustered distribution of the CD90$^+$ cells with both membrane and cytoplasm localization of CD90 expression (Figure 1A).

Serial transplantation was performed by subcutaneous injection of the CD90$^+$ cells isolated from tumor xenografts into a second and subsequently third batch of nude mice. Tumor nodules comparable to those isolated from HCC cell lines appeared after 2 months from the CD90$^+$ cells isolated from tumor xenografts (Table S2A). Flow cytometry showed a similar level of the CD90$^+$ cells in the first and second generation of tumor xenografts and HCC cell lines, suggesting a re-establishment of cellular hierarchy in tumors (Table S2B).

Further multimarker analyses revealed that the majority of CD90$^+$ cells in HCC cell lines also expressed CD44 (Figure 1Ba), a marker for HSPCs and an adhesion molecule that modulates tumor cell invasion and migration (Lara-Pezzi et al., 2001). To further characterize the CD90$^+$ subpopulations, two cell lines, MHCC97L and PLC (due to their differential distribution of the CD44$^+$ cells), were used to sort the CD90$^+$CD44$^+$ and CD90$^+$CD44$^-$ cells, which were injected subcutaneously into nude mice to assess tumorigenicity. Injection of the CD90$^+$CD44$^-$ cells at the number of 2,500 did not result in tumor formation after 4 months. When the injected cell number of the CD90$^+$CD44$^-$ cells was increased to 10,000, one mouse developed a tumor after 4 months. On the contrary, one mouse with 500 CD90$^+$CD44$^+$ cells developed a tumor nodule at 3 months, and 80% and 100% tumor development was observed with 2,500 and 10,000 CD90$^+$CD44$^+$ cells, respectively, at 2 months after cell injection (Table 2). The histology of tumor xenografts induced by the CD90$^+$CD44$^+$ and CD90$^+$ cells was similar. Immunofluorescent staining (IF) identified CD90$^+$CD44$^+$ cells in tumor specimens (Figure 1Bb).

Inhibition of CD44 Activity Induced CD90$^+$ Cell Apoptosis In Vitro and Suppressed CD90$^+$ Cell-Induced Local and Systemic Tumor Engraftments In Vivo

The role of CD44 expression in tumor cells was investigated by exposing the CD90$^+$ and CD90$^-$ cells from the MHCC97L and PLC cell lines with antihuman CD44 antibody at a range of concentrations for 24 hr. Inhibition of CD44 activity by administration of anti-CD44 antibody induced apoptosis of the CD90$^+$ and CD90$^-$ cells isolated from MHCC97L cell line in a dose-dependent manner. By comparison, blockade of CD44 activity in PLC cell line only induced the CD90$^+$ cells to undergo apoptosis and had a mild effect on the CD90$^-$ cells (Figure 2A).

The effect of CD44 blockade on tumor formation was further investigated in vivo. The CD90$^+$ cells from MHCC97L cell line were injected subcutaneously or directly into the liver of nude mice to generate local and metastatic tumor models, respectively. Different doses (5 mg/kg or 10 mg/kg, intravenous injection twice per week) of anti-CD44 antibody were administered

Table 2. Tumorigenic Capacity of the CD90$^+$ and CD90$^+$CD44$^+$ Cells from MHCC97L and PLC Cell Lines

Cell Lines	Phenotypes	No. of Injected Cells	No. of Mice with Tumor Formation/Total No. of Mice with Cell Injection (Range of Tumor Size [mm])		
			2 Months	3 Months	4 Months
MHCC97L	CD90$^+$	5×10^2	0/6	1/6 (3)	1/5 (2.5)
		2.5×10^3	3/5 (3–6)	2/2 (2.5–3)	
		1×10^4	5/5 (3–8)		
	CD90$^+$CD44$^+$	5×10^2	0/6	1/6 (4)	1/5 (3.5)
		2.5×10^3	4/5 (3–5)	1/1 (2.5)	
		1×10^4	5/5 (2–5)		
	CD90$^+$CD44$^-$	5×10^2	0/5	0/5	0/5
		2.5×10^3	0/5	0/5	0/5
		1×10^4	0/5	0/5	1/5 (2)
	total tumor cells	1×10^6	5/5 (3–7)		
PLC	CD90$^+$	5×10^2	0/5	0/5	0/5
		2.5×10^3	2/5 (2–5)	2/3 (2.5–3)	0/1
		1×10^4	4/5 (2–6)	1/1 (2)	
	CD90$^+$CD44$^+$	5×10^2	0/5	0/5	0/5
		2.5×10^3	3/5 (3–4)	1/2 (3)	0/1
		1×10^4	5/5 (2.5–5)		
	CD90$^+$CD44$^-$	5×10^2	0/5	0/5	0/5
		2.5×10^3	0/5	0/5	0/5
		1×10^4	0/5	0/5	1/5 (2)
	total tumor cells	1×10^6	4/5 (3–7)	1/1 (2)	

The sorted CD90$^+$ and CD90$^-$ cells, or CD90$^+$CD44$^+$ and CD90$^+$CD44$^-$ cells from different cell lines were injected subcutaneously into two different sites of a same mouse. Animals were sacrificed when tumor nodules were identified in nude mice, otherwise the mice were monitored continuously until the second or third time point.

into nude mice at the time of cell inoculation. In the absence of anti-CD44 antibody administration, the CD90$^+$ cells resulted in tumor formation subcutaneously in more than 80% of nude mice. Treatment with 5 mg/kg anti-CD44 antibody decreased the number of tumor-bearing mice, and 10 mg/kg further inhibited tumor formation (Figure 2B). Likewise, administration of anti-CD44 antibody also inhibited the engraftment of the CD90$^+$ cells (cell number = 1×10^4) isolated from other cell lines (Hep3B, PLC, and Huh7) (data not shown). In the tumor metastasis model, the CD90$^-$ cells from MHCC97L cell line did not generate liver and lung lesions. By comparison, 100% of mice developed liver lesion and lung metastasis 4 months after intrahepatic injection of 10,000 CD90$^+$ cells. In similar experiments, the isolated CD90$^+$CD44$^+$ cells induced comparable tumors in the liver and lung to the CD90$^+$ cells, whereas the CD90$^+$CD44$^-$ cells resulted in tumor formation in only 1 out of 6 mice at 4 months. Administration of anti-CD44 antibody prevented the formation of tumor nodules in the liver and lung induced by the CD90$^+$ cells (Figure 2Ca). A comparison of cell phenotypes in the primary and metastatic lesions using antibodies specifically targeting human CD44 and CD90 showed that, although the CD44 phenotype contributed to the majority of tumor cells in both types of lesions, which is consistent with the expression of CD44 in MHCC97L cell line, the metastatic tumors had a significantly higher proportion of CD90$^+$ and CD90$^+$CD44$^+$ cells than primary tumors (Figure 2Cb). The metastatic and primary tumors displayed similar histological features, and IHC confirmed an enrichment of the CD90$^+$ cells in metastatic nodules in the lung (Figure 2Cc).

Validation of Tumorigenic Properties of the CD45$^-$CD90$^+$ Cells Isolated from Human Tumor Specimens and Blood Samples

Based on the findings in HCC cell lines, CD90 was used as a marker to characterize CSCs in human tumor specimens, including 2 dysplastic nodules, 25 HCCs, and 3 intrahepatic cholangiocarcinomas (Cholangio Ca). The clinical data of liver cancer patients and controls is summarized in Table S3A. Since CD90 is also expressed by some lymphocytes, a combination of CD45$^-$CD90$^+$ was used to define nonlymphatic CD90$^+$ cells in tumor tissues. Flow cytometry revealed the presence of a small number (0%–0.03%) of CD45$^-$CD90$^+$ cells in normal, cirrhotic, and parallel nontumorous liver specimens. By comparison, the CD45$^-$CD90$^+$ cells (0.03%–6.2%) were detected in all the tumor specimens (Table S3b). Our findings are consistent with the reports of the CD90$^+$ cells at 0.01% in the normal adult liver (Nava et al., 2005), and higher levels in neoplastic tissues (Ceafalan et al., 2005). Multimarker analyses demonstrated that a proportion of CD45$^-$CD90$^+$ cells in tumor tissue concomitantly expressed stem cell markers, including CD44 (Figures 3Aa and 3Ab), CD133 (Table S3B), ESA, CXCR4, CD24, and KDR (Table S4). Interestingly, small numbers of CD45$^-$CD90$^+$ cells were also detected in one of the two dysplastic nodules, a precancerous stage of HCC (Table S3b).

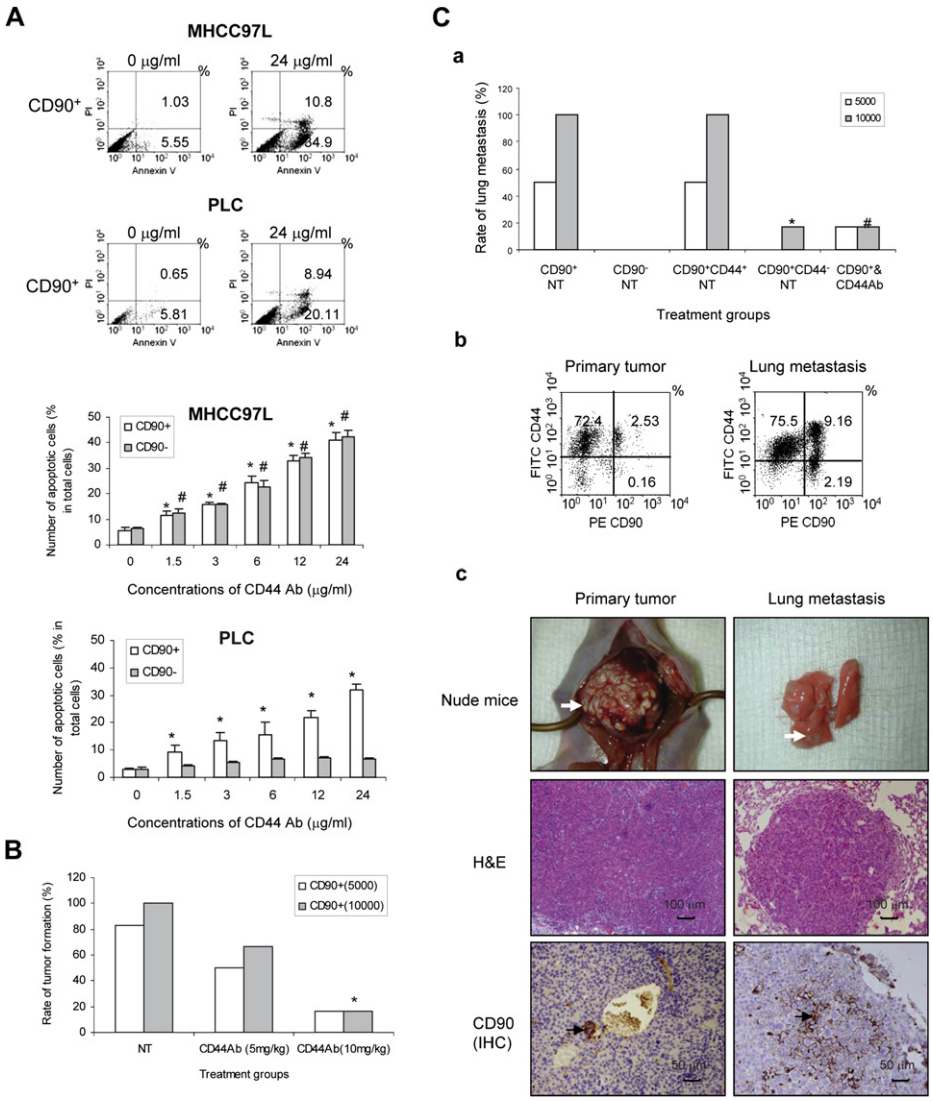

Figure 2. The Effect of CD44 Expression on the Biological Activity of the CD90$^+$ and CD90$^-$ Cells In Vitro and In Vivo

(A) The CD90$^+$ and CD90$^-$ cells were isolated from MHCC97L and PLC cell lines and seeded into 6-well culture plates. Different doses of anti-CD44 antibody (0, 1.5, 3, 6, 12, or 24 μg/ml) were added into the plate and incubated for 24 hr. The cells were labeled with Annexin V and PI and detected by a FACSCalibur. The dot plots represent typical features of Annexin V and PI staining. Treatment with anti-CD44 antibody induced a significant increase in cell apoptosis in both CD90$^+$ and CD90$^-$ cells isolated from MHCC97L cell line, but only the CD90$^+$ isolated from PLC cell line. *$p < 0.05$, compared with the CD90$^+$ cells without treatment (0 μg/ml anti-CD44 antibody); $^{\#}p < 0.05$, compared with the CD90$^-$ cells without treatment. The number of apoptotic cells is expressed as mean percentage ± SD from three independent experiments.

(B) Anti-CD44 antibody (5 mg/kg or 10 mg/kg twice per week, n = 6 in each group) was injected intravenously into BALB/c nude mice at the time of subcutaneous injection of the CD90$^+$ cells isolated from MHCC97L cell line. After 2 months, a decrease in the number of tumor-bearing mice was observed with anti-CD44 treatment. The bar chart shows tumor formation rates of different groups (n = 6 in each group). NT, no treatment. *$p < 0.05$, compared with NT.

(C) Phenotypically different cells isolated from MHCC97L cell line were injected orthotopically into the left lobe of the liver of BALB/c nude mice, respectively. Anti-CD44 antibody (10 mg/kg twice per week) was administered intravenously at the time of cell inoculation. After 4 months, animals were sacrificed to assess the formation of liver and metastatic lung lesions.

(Ca) The CD90$^-$ cells did not induce lung metastasis, whereas the CD90$^+$CD44$^+$ cells induced tumor nodules in the lung comparable to those induced by the CD90$^+$ cells. Anti-CD44 treatment decreased the number of lung nodules induced by the CD90$^+$ cells. The bar chart demonstrates tumor formation rates of different groups (n = 6 in each group). NT, no treatment. *$p < 0.05$, compared with the tumor formation rate induced by the CD90$^+$CD44$^+$ cells, NT; $^{\#}p < 0.05$, compared with the CD90$^+$ cells, NT.

(Cb) Flow cytometry using antibodies specifically targeting human CD44 and CD90 detected an enrichment of the CD90$^+$CD44$^+$ cells (9.16%) in lung lesions induced by the CD90$^+$ cells, compared to that of the primary tumor in the liver (2.53%).

(Cc) The photos display tumor nodules in the liver and lung of nude mice at 4 months after 10,000 CD90$^+$ cell injection. White arrows point to the primary tumor nodule in the liver and lung metastatic lesions, respectively. The histological features of the lung and primary tumor lesions are similar according to H&E staining. IHC shows an increase in the number of CD90$^+$ cells in the metastatic nodule. Black arrows indicate the CD90$^+$ cells in the primary and secondary tumors, respectively.

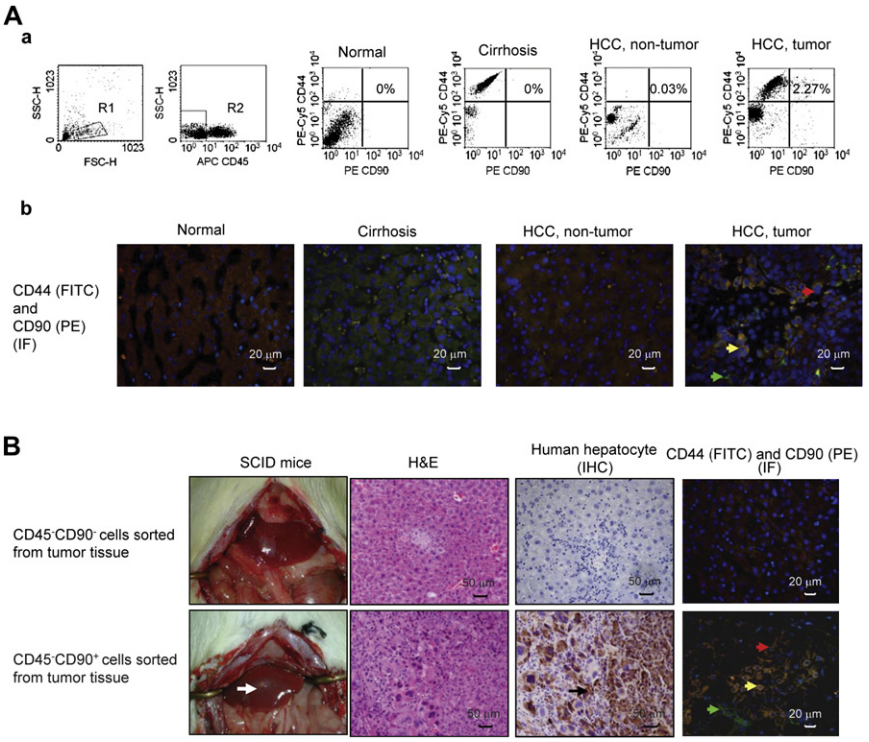

Figure 3. Tumorigenic Properties of the CD45$^-$CD90$^+$ Cells Isolated from Tumor Tissues

(Aa) Flow cytometry was performed to identify the CD45$^-$CD90$^+$ and CD45$^-$CD90$^+$CD44$^+$ cells in normal and cirrhotic liver, nontumorous, and tumor tissue samples. As our preliminary data showed that more than 90% of the CD90$^+$ cells were small in size, the CD45$^-$ cells were first gated from the small cell region (R1), and the CD90$^+$CD44$^+$ cells were then further analyzed in the CD45$^-$ region (R2). A distinct population of CD45$^-$CD90$^+$CD44$^+$ cells was detected in tumor tissue (2.27%), but not in normal (0%), cirrhotic (0%), or nontumorous liver samples (0.03%). The dot plots represent one sample in each group.

(Ab) The distribution of CD90$^+$ and CD44$^+$ cells in tumor tissue was confirmed by IF. Red, green, and yellow arrows indicate the CD90$^+$, CD44$^+$, and CD90$^+$CD44$^+$ cells, respectively.

(B) After dead cell removal, the CD45$^-$CD90$^+$ cells were isolated from tumor tissues with purity ranging from 78.9% to 84.8% and injected into the left lobe of the liver of SCID/Beige mice. The injected CD45$^-$CD90$^+$ cells, but not CD45$^-$CD90$^-$ cells, generated tumor nodules in the liver of SCID/Beige mice (a white arrow points to a tumor nodule) with a similar histology to that of the primary tumor. IHC of human hepatocyte recognized more than 90% positive cells in the generated tumor nodule. A black arrow indicates the cells expressing human hepatocyte antigen. By IF, the CD90$^+$CD44$^+$ cells were detected in the generated tumor tissues. Red, green, and yellow arrows indicate the CD90$^+$, CD44$^+$, and CD90$^+$CD44$^+$ cells, respectively.

Our preliminary data revealed that >80% viable cells were required for the in vivo tumorigenicity assay. Among the 28 tumor specimens collected, the cells isolated from 13 tumor specimens showed >80% cell viability, and these cells were then used for the in vivo tumorigenicity assay. After removal of dead cells, the CD45$^-$CD90$^+$ cells were isolated from individual tumor specimens using magnetic microbeads and injected orthotopically into the liver of individual severe-combined immunodeficient (SCID)/Beige mice. The isolated CD45$^-$ cells (total tumor cell control) from all the 13 tumor specimens formed tumor nodules in immunodeficient mice with the cell number of 1×10^6 at 4 months after cell injection. At 3 months, the CD45$^-$CD90$^+$ cells from seven tumor specimens formed tumor nodules with the cell number of 5,000, and after 4 months, the CD45$^-$CD90$^+$ cells from additional two tumor specimens developed tumor nodules with the cell number of 5,000, and one mouse developed a tumor nodule with 2,500 CD45$^-$CD90$^+$ cells. An extension of the observation time to 5 months did not increase the number of tumor-bearing mice. By comparison, when the cell number of the CD45$^-$CD90$^+$ cells was increased to 10,000, 100% of mice developed tumors within 4 months (Table 3). In contrast, the CD45$^-$CD90$^+$ cells isolated from normal, cirrhotic, and nontumorous liver tissues did not generate tumor nodules in SCID/Beige mice. Likewise, the CD45$^-$CD90$^-$ cells from tumor tissues did not develop tumor nodules, even after 5 months with 10,000 cells. Tumor xenografts displayed similar histological features to primary tumors in liver cancer patients. IHC using antihuman hepatocyte antibody, which specifically targets human antigens, detected more than 90% positive cells in tumor xenografts. In addition, IF detected CD90$^+$CD44$^+$ cells in the generated tumor tissues (Figure 3B).

Based on the clinical observation that tumor recurrence rate is high in HCC, even after curative hepatic resection or liver transplantation, we postulate that CSCs might be present in the circulation. To test this hypothesis, we investigated the number of CD45$^-$CD90$^+$ cells in blood samples by flow cytometry. A distinct population of CD45$^-$CD90$^+$ cells was identified in 33 out of 36 blood samples from liver cancer patients, but not in normal and cirrhosis controls. Consistent with the findings in tumor tissues, circulating CD45$^-$CD90$^+$ cells also concomitantly expressed CD44 (Figure 4A and Table S3B).

In the next series of experiments, the CD45$^-$CD90$^+$ cells were isolated from blood samples from 10 HCC patients and injected into the liver of SCID/Beige mice individually. At 4 months, the CD45$^-$ cells (bulk control; cell number = 1×10^6) from all the blood samples formed tumor nodules in immunodeficient mice. At the same observation time, tumor formation was also induced by 5,000 CD45$^-$CD90$^+$ cells isolated from blood sample of 5 HCC patients. When the cell number was increased to 10,000, circulating CD45$^-$CD90$^+$ cells from all HCC patients developed tumor nodules in the mice (Table 3). The generated tumor nodules displayed similar histological features to the primary tumors of liver cancer patients, and IHC revealed strong expression of human hepatocyte antigen in tumor xenografts. IF

showed the presence of $CD90^+CD44^+$ cells in the tumor nodules (Figure 4B).

Human $CD90^+$ cells were then isolated from tumor xenografts generated either by tumor tissue or circulating $CD45^-CD90^+$ cells and injected into the liver of a second and, subsequently, a third batch of SCID/Beige mice. In parallel experiments, the $CD90^+$ cells isolated from tumor xenografts displayed similar tumorigenic properties to the $CD45^-CD90^+$ cells isolated from tumor specimens or blood samples after 3 or 4 months (Table S2A). Flow cytometry detected a comparable number of human $CD90^+$ and $CD90^+CD44^+$ cells in the secondary and tertiary tumor xenografts, though the proportion of $CD90^+CD44^+$ cells within the pool of the $CD90^+$ cells was higher in tumor xenografts induced by circulating $CD45^-CD90^+$ cells than in tumors induced by tumor tissue $CD45^-CD90^+$ cells (Table S2C).

Statistical analysis was performed to investigate the correlation between the number of $CD45^-CD90^+$ cells in tumor specimens or blood samples and the clinicopathological parameters of liver cancer patients. No significant correlation was identified in the number of tumor tissue or circulating $CD45^-CD90^+$ cells and the gender, age (younger or older than 60 years), serum alpha-fetoprotein (AFP) level (lower or higher than 20 ng/ml), tumor grading, and staging according to the American Joint Committee on Cancer Tumor-Node-Metastasis. The number of circulating $CD45^-CD90^+$ cells was higher in patients with a tumor size larger than 5 cm than in patients with a smaller tumor ($1.47 \pm 2.46\%$ versus $0.15 \pm 0.27\%$, $p = 0.047$) (Table S5). Due to the limited number of cases and short follow-up period, the association between the number of tumor tissue or circulating $CD45^-CD90^+$ cells and disease-free survival or overall survival was not determined.

Differential Gene Expression Profiles Were Detected in the $CD45^-CD90^+$ Cells from Different Groups

Quantitative reverse transcriptase polymerase chain reaction (qRT-PCR) was used to compare gene expression profiles of the $CD45^-CD90^+$ and $CD45^-CD90^-$ cells isolated from tissue and blood samples of different groups. In tumor tissues, a significant upregulation of *CD44*, *Oct4*, *Bmi1*, *albumin*, and *AFP* mRNA was detected in the isolated $CD45^-CD90^+$ cells, compared with those sorted from normal, cirrhotic, and nontumorous liver tissues (Figure 5A). The $CD45^-CD90^+$ cells isolated from different groups expressed a comparable level of *Notch1* (Figure 5B). In contrast, the expression of *AFP*, *VIL2*, *MMP1*, and *JUNB* mRNA was significantly higher in the $CD45^-CD90^-$ cells sorted from tumor tissues, compared with those isolated from control tissues (Figure 5C). Finally, the expression of another group of genes, including *Wnt3a*, *signal transducers and activators of transcription 3* (*stat3*), and *hypoxia inducible factor-1*α (*HIF-1*α), was augmented in the $CD45^-CD90^+$ cells isolated from cirrhotic, nontumorous and tumor tissues, prominently from cirrhotic and nontumorous livers, compared with those from normal liver tissues (Figure 5D).

In the circulation, the $CD45^-CD90^+$ cells isolated from liver cancer patients expressed comparable levels of *Oct4*, *Bmi1*, *Notch1*, *Wnt3a*, *Stat3*, and *HIF-1*α mRNA to tumor tissue $CD45^-CD90^+$ cells, whereas circulating $CD45^-CD90^+$ cells expressed a higher level of *CD44* than those in tumor tissues. By comparison, a lower level of *albumin* and *AFP* mRNA was detected in circulating $CD45^-CD90^+$ cells than those in tumor tissues (Figure 5).

DISCUSSION

The present study reveals that CD90 is a potential marker for liver CSCs. This is supported by the finding that the number of $CD90^+$ cells isolated from all the HCC cell lines positively correlate with tumorigenicity and metastatic potentials of cell lines, and the $CD45^-CD90^+$ cells isolated from tumor tissues and blood samples of liver cancer patients have the capacity to generate tumor nodules in immunodeficient mice, whereas the $CD90^-$ or $CD45^-CD90^-$ cells do not. The maintenance of tumorigenicity of the $CD90^+$ cells following propagation into a second and, subsequently, a third batch of immunodeficient mice further supports CD90 as a marker for liver CSCs. Moreover, the $CD90^+$ and $CD45^-CD90^+$ cells reestablish the tumor cell hierarchy in immunodeficient mice. Together, these data provide evidence of the tumorigenicity and stem cell-like properties of the $CD90^+$ or $CD45^-CD90^+$ cells in human liver cancer.

Further characterization of the $CD90^+$ cells was performed by examining the expression of CD44, another stem cell marker, on these cells. Consistent with the distribution of the $CD45^-CD90^+$ cells in tumor specimens and blood, the $CD45^-CD90^+CD44^+$ cells were also detected locally and systemically in liver cancer patients. Therefore, we hypothesize that the expression of additional stem cell markers on the $CD90^+$ cells may represent different subpopulations of CSCs. A similar multimarker hypothesis has been suggested for CSCs in breast and pancreatic cancers (Al-Hajj et al., 2003; Li et al., 2007). CD44 is an adhesion molecule that regulates cell proliferation, migration, and invasion, by interaction with its ligands, heparanase, and hyaluronan, and, thus, plays an important role in tumor progression and metastasis (Götte and Yip, 2006). Our preliminary results showed that the sorted $CD44^+$ cells from MHCC97L and PLC cell lines developed tumor nodules in nude mice faster than the $CD44^-$ cells (Table S6), supporting the role of CD44 in tumor progression. However, the presence of $CD45^-CD44^+$ cells in cirrhotic liver tissues (Figure 3A) hinders its application as a specific marker for liver CSCs when used alone. The $CD90^+CD44^+$ phenotype of liver CSCs might explain the aggressive growth pattern of HCC. In addition, blockade of CD44 activity inhibited the survival of the $CD90^+$ cells in vitro and prevented tumor engraftment in vivo, thereby highlighting CD44 as a therapeutic target for the $CD90^+$ CSCs. Administration of anti-CD44 antibody had a more pronounced effect on apoptosis of MHCC97L cells (inducing both $CD90^+$ and $CD90^-$ cells undergoing apoptosis) than PLC cells (only inducing $CD90^+$ cells undergoing apoptosis). This finding supports the observation that both $CD90^+$ and $CD90^-$ cells in MHCC97L cell line concomitantly express CD44, whereas only a small proportion of the $CD90^-$ cells in PLC cell line concomitantly express CD44. The effect of CD44 expression on the $CD90^-$ cells remains to be explored. However, as the $CD90^-$ cells are not tumorigenic, while CD44 is only highly expressed by the $CD90^-$ cells in the cell lines with metastatic properties, we postulate that CD44 expression on the $CD90^-$ cells might contribute to the maintenance of metastatic properties of CSCs when they are dividing into adult phenotypes. As cell viability is a major factor affecting tumor formation, especially after multiple-step sorting procedures using magnetic microbeads, we did not specifically investigate the tumorigenicity of the $CD45^-CD90^+CD44^+$ and $CD45^-CD90^+CD44^-$ cells from tumor tissues or blood

Table 3. Tumorigenic Capacity of the CD45$^-$CD90$^+$ Cells from Tumor Specimens and Blood Samples of Liver Cancer Patients

Patient No.	Sample Type	% of CD45$^-$CD90$^+$ Cells	No. of Injected Cells	No. of Mice with Tumor Formation/Total No. of Mice with Cell Injection (Range of Tumor Size [mm])			Patient No.	Sample Type	% of CD45$^-$CD90$^+$ Cells	No. of Injected Cells	No. of Mice with Tumor Formation/Total No. of Mice with Cell Injection (Range of Tumor Size [mm])		
				3 Months	4 Months	5 Months					3 Months	4 Months	5 Months
1	tumor	2.56	2.5×10^3	0/2	0/2	0/2	1	blood	0.1	1×10^3	0/2	0/2	0/2
			5×10^3	1/2 (3.5)	0/1	0/1				5×10^3	0/2	1/2 (2)	0/1
			1×10^4	2/2 (6–7)						1×10^4	0/2	1/2 (3.5)	0/1
2	tumor	3.4	2.5×10^3	0/2	0/2	0/2	3	blood	1.42	1×10^3	0/2	0/2	0/2
			5×10^3	0/2	0/2	0/2				5×10^3	0/2	1/2 (2.5)	0/1
			1×10^4	1/2 (2)	0/1	0/1				1×10^4	0/2	1/2 (2.5)	1/1 (2.3)
3	tumor	3.89	2.5×10^3	0/2	0/2	0/2	4	blood	3.45	1×10^3	0/2	0/2	0/2
			5×10^3	2/2 (1.8–4)						5×10^3	0/2	2/2 (2–2.5)	
			1×10^4	2/2 (6–8)						1×10^4	0/2	2/2 (1.5–3.5)	
4	tumor	6.2	2.5×10^3	0/2	1/2 (2)	0/1	5	blood	0.49	1×10^3	0/2	0/2	0/2
			5×10^3	2/2 (2.5–4)						5×10^3	0/2	1/2 (2)	0/1
			1×10^4	2/2 (6.5–8)						1×10^4	0/2	2/2 (2–3)	
5	tumor	1.51	2.5×10^3	0/2	0/2	0/2	7	blood	0.9	1×10^3	0/2	0/2	0/2
			5×10^3	2/2 (5–8)						5×10^3	0/2	0/2	0/2
			1×10^4	2/2 (7–8)						1×10^4	0/2	1/2 (3.2)	1/1 (1.8)
6	tumor	1.83	2.5×10^3	0/2	0/2	0/2	9	blood	0.08	1×10^3	0/2	0/2	0/2
			5×10^3	1/2 (4)	0/1	0/1				5×10^3	0/2	0/2	0/2
			1×10^4	1/2 (5.3)	0/1	0/1				1×10^4	0/2	1/2 (2.7)	0/1
7	tumor	2.34	2.5×10^3	0/2	0/2	0/2	11	blood	0.4	1×10^3	0/2	0/2	0/2
			5×10^3	0/2	1/2 (1.5)	0/1				5×10^3	0/2	0/2	0/2
			1×10^4	0/2	1/2 (2.5)	0/1				1×10^4	0/2	2/2 (3.2–3.5)	
8	tumor	0.74	2.5×10^3	0/2	0/2	0/2	13	blood	0.13	1×10^3	0/2	0/2	0/2
			5×10^3	0/2	1/2 (2)	0/1				5×10^3	0/2	2/2 (2–2.5)	
			1×10^4	0/2	1/2 (2.2)	0/1				1×10^4	0/2	2/2 (2.8–3.3)	
9	tumor	4.14	2.5×10^3	0/2	0/2	0/2	14	blood	0.04	1×10^3	0/2	0/2	0/2
			5×10^3	0/2	0/2	0/2				5×10^3	0/2	0/2	0/2
			1×10^4	1/2 (3.8)	0/1	0/1				1×10^4	0/2	1/2 (2.9)	0/1
10	tumor	2.51	2.5×10^3	0/2	0/2	0/2	15	blood	0.07	1×10^3	0/2	0/2	0/2
			5×10^3	1/2 (3.4)	0/1	0/1				5×10^3	0/2	0/2	0/2
			1×10^4	1/2 (5)	0/1	0/1				1×10^4	0/2	2/2 (3–3.5)	
11	tumor	2.24	2.5×10^3	0/2	0/2	0/2							
			5×10^3	0/2	0/2	0/2							
			1×10^4	1/2 (6.4)	0/1	0/1							

Table 3. *Continued*

Patient No.	Sample Type	% of $CD45^-CD90^+$ Cells	No. of Injected Cells	No. of Mice with Tumor Formation/Total No. of Mice with Cell Injection (Range of Tumor Size [mm])			Patient No.	Sample Type	% of $CD45^-CD90^+$ Cells	No. of Injected Cells	No. of Mice with Tumor Formation/Total No. of Mice with Cell Injection (Range of Tumor Size [mm])		
				3 Months	4 Months	5 Months					3 Months	4 Months	5 Months
12	tumor	0.79	2.5×10^3	0/2	0/2	0/2							
			5×10^3	1/2 (5.2)	0/1	0/1							
			1×10^4	2/2 (4.8–7)									
13	tumor	3.03	2.5×10^3	0/2	0/2	0/2							
			5×10^3	0/2	0/2	0/2							
			1×10^4	0/2	1/2 (3)	0/1							

The % of $CD45^-CD90^+$ cells was analyzed in total cell population. A same number of isolated $CD45^-CD90^+$ cells from each patient were injected into the liver of two individual SCID/Beige mice. Animals were sacrificed when tumor nodules were identified in the mouse liver at the indicated time points by laparotomy; otherwise, the mice were monitored continuously until the second or third time point. Tumorigenic capacity was defined when tumor nodules were identified in either one of the two mice with cell injection.

samples. Instead, flow cytometry and IF were used to confirm the presence of $CD90^+CD44^+$ cells in the generated tumor xenografts, and the data were consistent with the findings in HCC cell lines.

Though both types of cells could generate tumors in immunodeficient mice, different genetic characteristics were identified between tumor tissue and circulating $CD45^-CD90^+$ cells. While both highly expressed stem cell markers, *Oct4*, *Bmi1*, and *Wnt3a*, tumor tissue $CD45^-CD90^+$ cells expressed a higher level of tissue specific markers, *albumin* and *AFP*. On the other hand, circulating $CD45^-CD90^+$ cells expressed a higher level of CD44 than the tumor tissue counterpart, suggesting that circulating CSCs might harbor a more potent capacity to migrate and settle in the target organs. The present study suggests that tumor tissue $CD45^-CD90^+$ cells are a source of the circulating counterpart, as we have detected a decreased number of circulating $CD45^-CD90^+$ cells after hepatic resection (data not shown). In addition, a higher number of circulating $CD45^-CD90^+$ cells were detected in the patients with a larger tumor size, suggesting a positive correlation between the presence of circulating CSCs and disease progression.

In our study, very low levels of $CD45^-CD90^+$ cells are also present in normal and cirrhotic liver tissues, and this finding is consistent with others' findings (Fiegel et al., 2003; Isabel et al., 2006; Corcelle et al., 2006). Therefore, an investigation of the differences between the $CD45^-CD90^+$ cells isolated from tumor specimens or blood samples of liver cancer patients and those from normal or cirrhotic liver tissues may provide important clues to understand the mechanism underlying hepatocarcinogenesis. By qRT-PCR using specific primers, we have detected the augmentation of *Oct4* and *Bmi1*, which modulate stem cell self-renewal and multipotency, in tumor tissue and circulating $CD45^-CD90^+$ cells from liver cancer patients, thereby providing evidence of the stem cell nature of these cells and their potential role in hepatocarcinogenesis (Campbell et al., 2007; Bruggeman et al., 2007). A comparable level of *Notch1* expressed by both normal hepatic and tumor tissue $CD45^-CD90^+$ cells indicates their similarity as stem cells (Chiba, 2006), signifying that this gene might not play a prominent role in hepatocarcinogenesis. The enhanced expression of *CD44* in tumor specimens, and a greater enhancement in circulating $CD45^-CD90^+$ cells, confirmed our data obtained from flow cytometry. The upregulation of *AFP* and *albumin* in tumor tissue $CD45^-CD90^+$ cells confirms these cells as originating from the liver (Colli et al., 2006; Alison, 2006). The increased expression of *VIL2*, *MMP1*, and *JUNB* in tumor tissue $CD45^-CD90^-$ cells implies a role of these genes in the differentiation of CSCs into adult phenotypes (Curto and McClatchey, 2004; Seiki, 2003; Jochum et al., 2001). Lastly, the expression of another group of genes, *Wnt3a*, *Stat3*, and *HIF-1*α, was upregulated in the $CD45^-CD90^+$ cells isolated from cirrhotic livers, nontumorous and tumor specimens, and blood samples of liver cancer patients. This finding, and the observation that upregulation was most prominent in cirrhotic and nontumorous livers, implies a potential role of these genes in linking chronic injury to hepatocarcinogenesis (Lee et al., 2006; Kim et al., 2007; Paul et al., 2004; Yang et al., 2004a).

Using an antibody specifically targeting murine CD90, we detected an increasing proportion of murine $CD90^+$ cells in secondary and tertiary tumor xenografts (data not shown). This result

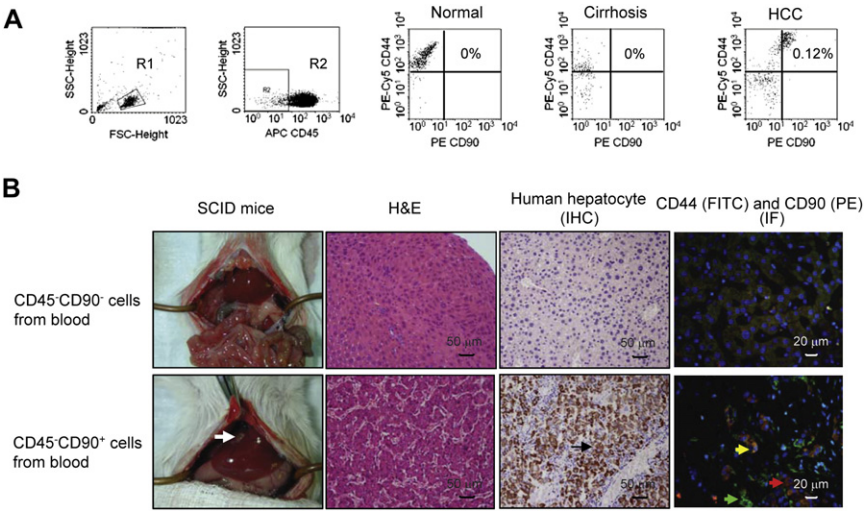

Figure 4. Tumorigenicity of the CD45$^-$CD90$^+$ Cells Isolated from Blood Samples of Liver Cancer Patients

(A) More than 90% of the CD90$^+$ cells isolated from blood samples were identified in the small cell region. Using the same protocol to analyze the flow cytometry data as that in tumor tissues, the CD45$^-$CD90$^+$CD44$^+$ cells were detected in the blood sample from liver cancer patients (0.12%), but not in the normal (0%) and cirrhosis controls (0%). The dot plots represent one sample in each group, respectively.

(B) The CD45$^-$CD90$^+$ and CD45$^-$CD90$^-$ cells were isolated from blood samples of liver cancer patients, with purity ranging from 81.9% to 84.5%, and injected into the left lobe of the liver of SCID/Beige mice. The isolated CD45$^-$CD90$^+$ cells, but not CD45$^-$CD90$^-$ cells, formed tumor nodules in the liver of SCID/Beige mice. The white arrow indicates a tumor nodule. H&E staining of generated tumor nodules revealed a poorly differentiated HCC. IHC detected more than 90% positive cells stained with the anti-human hepatocyte antibody. The black arrow indicates the cells expressing human hepatocyte antigen. IF recognized both CD90$^+$ and CD44$^+$ cells in tumor xenograft. Red, green, and yellow arrows indicate the CD90$^+$, CD44$^+$, and CD90$^+$CD44$^+$ cells, respectively.

suggests the formation of cell-cell fusions of human and murine cells during the growth of human tumor in immunodeficient mice. However, IHC studies using an antibody specifically targeting human hepatocyte antigen demonstrated that more than 90% of cells in tumor xenografts were human origin. Flow cytometry using anti-human and anti-murine CD90 antibodies revealed that <0.5% of the total cell population was double positive. These results indicate that the proportion of cell-cell fusion in tumor xenografts is low. We hypothesize that the murine CD90$^+$ cells favor the survival, self-renewal, differentiation, and metastasis of human CSCs mainly through participation in the establishment of a microenvironment (Gilbertson and Rich, 2007; Karnoub et al., 2007), rather than direct integration with human cells.

The present study has shown the presence of local and circulating tumorigenic CD45$^-$CD90$^+$, and an aggressive subpopulation of CD90$^+$CD44$^+$ CSCs in human liver cancer. Due to the small number of cases and short follow-up period, detailed statistical analyses could not be performed to evaluate the correlation between the number of CSCs and clinico-pathological features of liver cancer patients. The universal presence of the CD45$^-$CD90$^+$ cells in tumor tissues and more than 90% of blood samples and a positive correlation between the number of circulating CD45$^-$CD90$^+$ cells and tumor size suggests that circulating CSCs could reflect tumor status and provide a cellular marker for disease surveillance. In addition, the detectable levels of circulating CD45$^-$CD90$^+$ cells in patients with small tumors (<5 cm) and dysplastic nodules reveal an important role of these CD45$^-$CD90$^+$ cells in early stage hepatocarcinogenesis. Finally, the finding that inhibition of CD44 induces the death of CD90$^+$ cells and prevents tumor engraftments both locally and systemically highlights the potential of targeting CD90$^+$CD44$^+$ CSCs for tumor eradication in future therapeutic strategies.

EXPERIMENTAL PROCEDURES

Cell Lines

Human cell lines, MIHA (kindly provided by Dr. J. Roy-Chowdhury [Brown et al., 2000]), HepG2, Hep3B, PLC, Huh7 (ATCC, Manassas, VA), MHCC97L, and MHCC97H (HCC cell lines with low to high metastatic properties, respectively [Tang et al., 2004]), were maintained as monolayer cultures in high glucose Dulbecco's Modified Eagle Medium (DMEM) with 10% fetal bovine serum (FBS) and 1% penicillin (Life Technologies, Carlsbad, CA) at 37°C in a humidified atmosphere of 5% CO_2 in air.

Patients and Sample Collection

Two patients with dysplastic nodules (2/2 were liver transplantation recipients) and 36 patients with liver tumors who had undergone laparotomy (24/36 had curative hepatic resection, 4/36 received liver transplantation, and 8/36 had liver biopsy) were recruited in this study. Pathological diagnosis was made according to the histology of tumor specimens or biopsy and examined by experienced pathologists. Nineteen patients with cirrhosis (10/19 received liver transplantation) and 19 normal subjects (10/19 were liver donors) were used as controls. The diagnosis of cirrhosis was made according to histological findings in liver explants or CT/MRI scan results. The majority of patients with HCC (28/36) and cirrhosis (15/19) were positive for serum hepatitis B surface antigen (HBsAg). All tissue and blood samples were obtained from consenting patients and approved by the Institutional Review Board of the University of Hong Kong. The clinical data for the above patients and controls are summarized in Table S3.

Tumor, parallel nontumorous, cirrhotic, and normal liver tissues were harvested at the time of operation and placed into DMEM medium. The procedure of cell isolation from liver tissues was performed as previously described (Yang et al., 2004b) with some modifications. In brief, after digestion with type IV collagenase (100 units/ml) (Sigma-Aldrich, St. Louis, MO) at 37°C for 15 min, tissues were minced and cell suspension was passed through a 40 μM nylon mesh. After lysis of red blood cells, cells were counted and subjected to flow cytometry analysis or cell sorting.

Before the operation, 10 ml of EDTA blood were collected from patients and controls. Mononuclear cells were isolated from the EDTA blood using Ficoll-Paque PLUS (Amersham Bioscience, Buckinghamshire, England) density gradient centrifugation before proceeding to flow cytometry analysis or cell sorting.

Flow Cytometry

The isolated cells from HCC cell lines, tissue, and blood samples were labeled with the following anti-human antibodies: FITC-ESA, FITC-CD44, PE-CD15, PE-CD24, PE-CD30, PE-CD32, PE-CD33, PE-CD38, PE-CD56, PE-CD59, PE-CK19, PE-CD117, PE-KDR, purified or PE-CD90, APC-CD45, APC-CD34 (BD Biosciences PharMingen, San Diego, CA), PE-Cy5-CD44, PE-Cy5-CXCR4 (eBioscience, San Diego, CA), and PE-CD133 (Miltenyi Biotech Inc, Bergisch Gladbach, Germany). Labeled cells were detected using a FACSCalibur

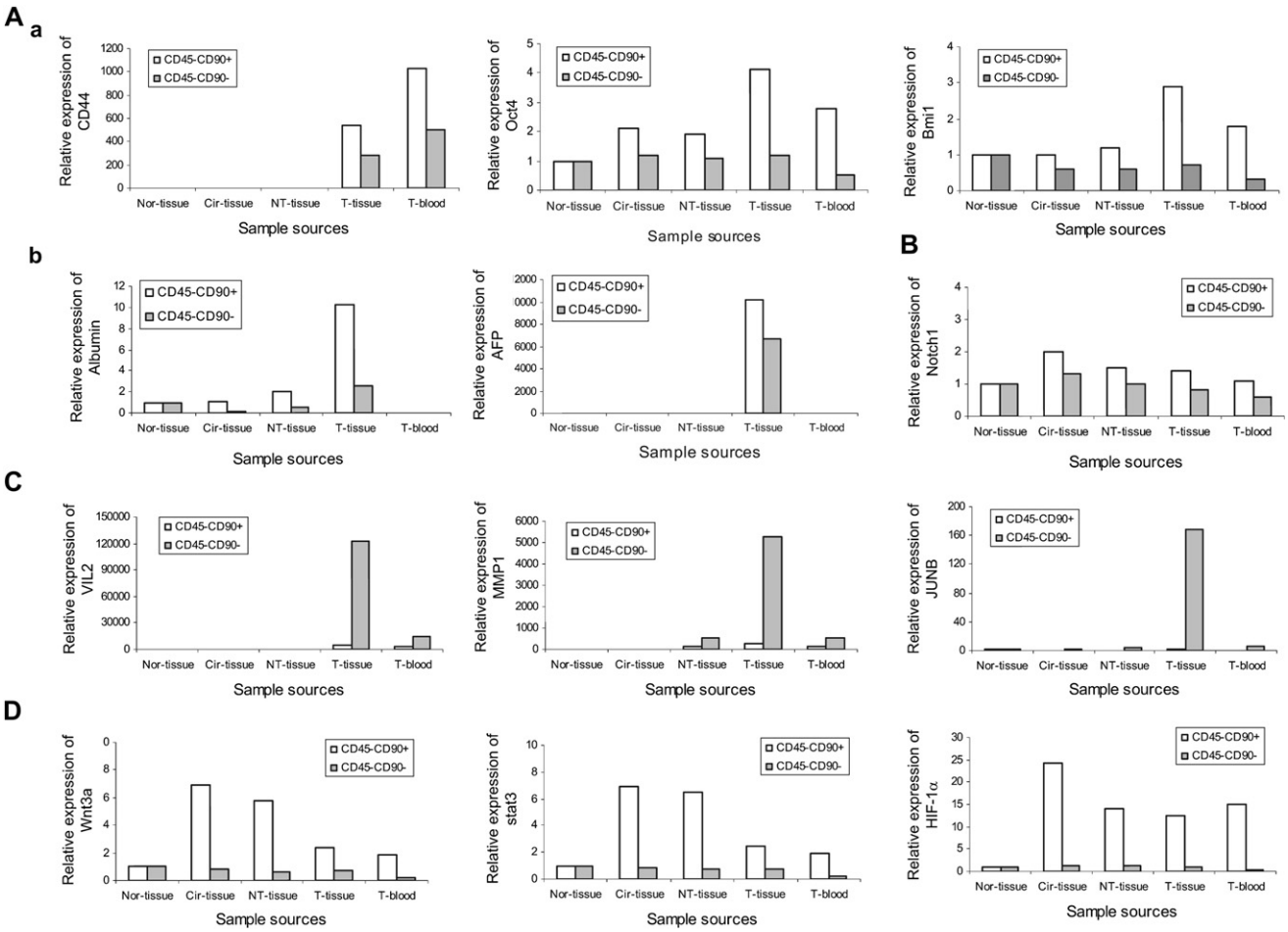

Figure 5. Differential Gene Expression of the CD45$^-$CD90$^+$ and CD45$^-$CD90$^-$ Cells Isolated from Tissue and Blood Samples of Different Groups, Assessed by Using Quantitative Reverse Transcriptase Polymerase Chain Reaction

(Aa) The expression of *CD44*, *Oct4*, and *Bmi1* was specifically upregulated in the CD45$^-$CD90$^+$ cells isolated from tumor tissues and blood samples of liver cancer patients, compared with that in the CD45$^-$CD90$^+$ cells isolated from normal livers. In addition, *CD44* expression was even higher in the circulating CD45$^-$CD90$^+$ cells than the tumor tissue counterpart.

(Ab) The expression of *albumin* and *AFP* was specifically upregulated in the CD45$^-$CD90$^+$ cells isolated from tumor tissues, compared with that in the CD45$^-$CD90$^+$ cells sorted from normal liver tissues.

(B) The CD45$^-$CD90$^+$ cells isolated from normal and cirrhotic livers, tumor tissues, and blood samples of liver cancer patients expressed a comparable level of *Notch1*.

(C) The expression of *VIL2*, *MMP1*, and *JUNB* was exclusively upregulated in the CD45$^-$CD90$^-$ cells isolated from tumor tissues, compared with that in the CD45$^-$CD90$^-$ cells sorted from normal liver tissues.

(D) The expression of *Wnt3a*, *Stat3*, and *HIF-1*α was augmented in the CD45$^-$CD90$^+$ cells isolated from cirrhotic livers, nontumorous and tumor tissues, and blood samples from liver cancer patients. The data present at least five samples in each group. Nor, normal liver; Cir, cirrhotic liver; NT, nontumorous; T, tumor; T-blood, blood samples from liver cancer patients.

(Becton Dickinson Immunocytometry Systems, San Jose, CA). Appropriate isotypes of nonrelated antibodies were used as controls. A dead cell removal procedure was performed before antibody labeling and flow cytometry analysis.

Cell Sorting

Cocktail PE-conjugated mouse anti-human CD90 and FITC-conjugated anti-human CD44 antibody were made according to the manufacturer's instructions (StemCell Technologies Inc., Miami, Florida). The cells from MHCC97L or PLC cell lines were suspended in PBS with 2% FBS and 0.5 μM EDTA, sequentially labeled with anti-CD90 and anti-CD44 antibody cocktail, and mixed with magnetic microbeads. The CD90$^+$ and CD90$^-$ cells, and subsequent CD90$^+$CD44$^+$ and CD90$^+$CD44$^-$ cells, were then separated using a magnet. The purity of sorted cells was evaluated by flow cytometry. For the isolation of cells from tumor specimens and blood samples, a modified protocol was performed, including dead cell removal and subsequent two-step separation procedure involving CD45 depletion and CD90 selection (Miltenyi Biotech Inc). The tumorigenicity of CD45$^-$CD90$^+$ cells isolated from tumor tissues or blood was characterized by injecting the sorted cells into immunodeficient mice. The viability of sorted cells was assessed by trypan blue staining, and >80% cell viability was set as the requirement for the in vivo tumorigenicity assay.

Tumor Xenografts in BALB/c Nude Mice or SCID/Beige Mice

Male BALB/c nude mice and SCID/Beige mice, aged 4 to 5 weeks, were purchased from the Animal Laboratory Unit of the University of Hong Kong. The mice were maintained under standard conditions and cared for according to the institutional guidelines for animal care. All the animal experiments were

approved by the Committee on the Use of Live Animals in Teaching and Research of the University of Hong Kong. The tumor cells from HCC cell lines have the capacity to generate tumor nodules on the back of BALB/c nude mice (Tian et al., 1999). Hence, the $CD90^+$ and $CD90^-$ cells isolated from different HCC cell lines were injected subcutaneously into two sides of the same nude mouse, respectively, for controlled visualization and comparison. To favor cell growth, the cells isolated from human tumor tissues and blood samples were injected orthotopically into the left lobe of the liver of SCID/Beige mice as previously described (Yang et al., 2005). To generate a metastatic tumor model, the sorted $CD90^+$, $CD90^-$, $CD90^+CD44^+$, and $CD90^+CD44^-$ cells isolated from MHCC97L cell line were injected orthotopically into the liver of different BALB/c nude mice. A total of 1×10^6 tumor cells were injected into immunodeficient mice to serve as a control of cell viability. Animals were sacrificed at the indicated time intervals when tumor nodules were identified on the body surface of nude mice or in the liver of SCID/Beige mice by laparotomy. If tumors were not identified, the abdominal incision was closed by sutures, and the mice were monitored until the second or third time point. In the tumor metastasis model, animals were sacrificed at 4 months after cell injection to investigate the formation of liver and lung lesions.

Blockade of CD44 Activity In Vitro and In Vivo

For in vitro experiments, the $CD90^+$ and $CD90^-$ cells isolated from HCC cell lines were treated for 24 hr with different doses (0, 1.5, 3, 6, 12, or 24 μg/ml) of anti-human CD44 antibody (International Blood Group Reference Laboratory, Bristol, England). The cells were then labeled with Annexin-V and Propidium iodide (PI) (BD Biosciences PharMingen) and detected in a FACSCalibur (Becton Dickinson Immunocytometry Systems).

For in vivo experiments, 5,000 or 10,000 $CD90^+$ cells were isolated from HCC cell line and injected subcutaneously into BALB/c nude mice. In the lung metastasis model, the $CD90^+$ and $CD90^-$ cells were isolated from MHCC97L cell line and injected into the left lobe of the liver of BALB/c nude mice, respectively. At the time of cell inoculation, anti-human CD44 antibody was administered intravenously (5 mg/kg or 10 mg/kg twice per week). The mice were monitored continuously for signs of subcutaneous tumor formation, or sacrificed at 4 months to investigate tumor formation in the liver and lung.

Histological Studies

The embedded tissues were cut into 5 μm-thick sections for histological analyses by H&E staining, IHC to detect CD90 and human hepatocytes (Dako, Glostrup, Denmark), and IF to examine CD44 and CD90 expression. The anti-human hepatocyte antibody recognizes human liver tumors by IHC (Minervini et al., 1997). Our preliminary investigations showed that the anti-human hepatocyte antibody did not crossreact with murine antigen. Sections were incubated sequentially with primary and secondary antibodies for 1 hr at room temperature. Counter-staining of the nucleus was performed using hematoxylin and DAPI for IHC and IF, respectively.

Real-Time Quantitative Reverse Transcriptase Polymerase Chain Reaction

Total RNA was extracted from the isolated $CD45^-CD90^+$ and $CD45^-CD90^-$ cells from tissue or blood using the RNeasy RNA Mini Kit (QIAGEN Inc., Valencia, CA). RNA was resuspended in 30 μl RNase-free water. First strand cDNA was synthesized by using ImProm-II reverse transcriptase (Promega, Madison, WI). Real-time qPCR was performed using the first strand cDNA, 10 μM forward and reverse primers, and the SYBR Green PCR master mix. The primer sequences and PCR conditions are summarized in Table S7. The reactions were performed using the ABI PRISM 7700 Sequence Detector (Applied Biosystems, Foster City, CA). Fluorescence signals were analyzed using SDS 1.9.1 software (Applied Biosystems). Expression levels were calculated as the relative expression ratio compared to β-actin. Since the $CD45^-CD90^+$ cells could only be isolated from tissue, but not blood, samples of normal and cirrhosis controls, a comparison of gene expression profiles was performed between the $CD45^-CD90^+$ or $CD45^-CD90^-$ cells isolated from tumor and control tissues and between the $CD45^-CD90^+$ or $CD45^-CD90^-$ cells isolated from blood samples of liver cancer patients and those isolated from tumor specimens. As the number of isolated cells was usually small, following confirmation of cell purity, at least five samples from each source were pooled together to obtain reliable gene expression data.

Statistical Analysis

Comparison of apoptotic cell number and tumor formation rate with different treatments, and the number of tumor tissue and circulating $CD45^-CD90^+$ cells in different tumor size groups, were performed using Student's t test. SPSS software (version 12.0 for Windows; SPSS Inc., Chicago, IL) was used for all statistical analyses. A p value less than 0.05 was considered statistically significant.

Supplemental Data

The Supplemental Data include seven supplemental tables and can be found with this article online at http://www.cancercell.org/cgi/content/full/13/2/153/DC1/.

ACKNOWLEDGMENTS

The immortalized nontumorigenic normal human hepatocyte cell line (MIHA) was kindly provided by Dr J. Roy-Chowdhury, Albert Einstein College of Medicine, New York, USA. The MHCC97L and MHCC97H cell lines were a kind gift from Prof. Zhao-You Tang from the Liver Cancer Institute, Zhongshan Hospital, Fudan University, Shanghai, P.R. China. This study was supported by the Sun Chieh Yeh Research Foundation for Hepatobiliary and Pancreatic Surgery and the Mrs. Li Ka Shing Fund of the University of Hong Kong.

Received: August 5, 2007
Revised: November 10, 2007
Accepted: January 14, 2008
Published: February 4, 2008

REFERENCES

Al-Hajj, M., Wicha, M.S., Benito-Hernandez, A., Morrison, S.J., and Clarke, M.F. (2003). Prospective identification of tumorigenic breast cancer cells. Proc. Natl. Acad. Sci. USA *100*, 3983–3988.

Alison, M.R. (2006). Liver cancer: A disease of stem cells? Panminerva Med. *48*, 165–174.

Arii, S., Yamaoka, Y., Futagawa, S., Inoue, K., Kobayashi, K., Kojiro, M., Makuuchi, M., Nakamura, Y., Okita, K., and Yamada, R. (2000). Results of surgical and nonsurgical treatment for small-sized hepatocellular carcinomas: a retrospective and nationwide survey in Japan. The Liver Cancer Study Group of Japan. Hepatology *32*, 1224–1229.

Brown, J.J., Parashar, B., Moshage, H., Tanaka, K.E., Engelhardt, D., Rabbani, E., Roy-Chowdhury, N., and Roy-Chowdhury, J. (2000). A long-term hepatitis B viremia model generated by transplanting nontumorigenic immortalized human hepatocytes in Rag-2-deficient mice. Hepatology *31*, 173–181.

Bruggeman, S.W., Hulsman, D., Tanger, E., Buckle, T., Blom, M., Zevenhoven, J., van Tellingen, O., and van Lohuizen, M. (2007). Bmi1 controls tumor development in an ink4a/arf-independent manner in a mouse model for glioma. Cancer Cell *12*, 328–341.

Campbell, P.A., Perez-Iratxeta, C., Andrade-Navarro, M.A., and Rudnicki, M.A. (2007). Oct4 targets regulatory nodes to modulate stem cell function. PLoS ONE. *2*, e553.

Ceafalan, L., Vidulescu, C., Radu, E., Regalia, T., Popescu, I., Pana, M., Serghei, L., Voiculescu, B., and Popescu, L.M. (2005). Expression of stem cell markers on fetal and tumoral human liver cells in primary culture. Rev. Med. Chir. Soc. Med. Nat. Iasi *109*, 96–104.

Chiba, S. (2006). Notch signaling in stem cell systems. Stem Cells *24*, 2437–2447.

Cho, R.W., Wang, X., Diehn, M., Shedden, K., Chen, G.Y., Sherlock, G., Gurney, A., Lewicki, J., and Clarke, M.F. (2007). Isolation and Molecular Characterization of Cancer Stem Cells in MMTV-Wnt-1 Murine Breast Tumors. Stem Cells, in press. Published online November 7, 2007.

Colli, A., Fraquelli, M., Casazza, G., Massironi, S., Colucci, A., Conte, D., and Duca, P. (2006). Accuracy of ultrasonography, spiral CT, magnetic resonance,

and alpha-fetoprotein in diagnosing hepatocellular carcinoma: A systematic review. Am. J. Gastroenterol. *101*, 513–523.

Collins, A.T., Berry, P.A., Hyde, C., Stower, M.J., and Maitland, N.J. (2005). Prospective identification of tumorigenic prostate cancer stem cells. Cancer Res. *65*, 10946–10951.

Corcelle, V., Stieger, B., Gjinovci, A., Wollheim, C.B., and Gauthier, B.R. (2006). Characterization of two distinct liver progenitor cell subpopulations of hematopoietic and hepatic origins. Exp. Cell Res. *312*, 2826–2836.

Curto, M., and McClatchey, A.I. (2004). Ezrin…a metastatic detERMinant? Cancer Cell *5*, 113–114.

Dan, Y.Y., Riehle, K.J., Lazaro, C., Teoh, N., Haque, J., Campbell, J.S., and Fausto, N. (2006). Isolation of multipotent progenitor cells from human fetal liver capable of differentiating into liver and mesenchymal lineages. Proc. Natl. Acad. Sci. USA *103*, 9912–9917.

Dennis, J.E., Esterly, K., Awadallah, A., Parrish, C.R., Poynter, G.M., and Goltry, K.L. (2007). Clinical-scale Expansion of a Mixed Population of Bone Marrow Derived Stem and Progenitor Cells for Potential Use in Bone Tissue Regeneration. Stem Cells *25*, 2575–2582.

El-Serag, H.B. (2004). Hepatocellular carcinoma: Recent trend in the United States. Gastroenterology *127*, S27–S34.

Fiegel, H.C., Park, J.J., Lioznov, M.V., Martin, A., Jaeschke-Melli, S., Kaufmann, P.M., Fehse, B., Zander, A.R., and Kluth, D. (2003). Characterization of cell types during rat liver development. Hepatology *37*, 148–154.

Gilbertson, R.J., and Rich, J.N. (2007). Making a tumour's bed: Glioblastoma stem cells and the vascular niche. Nat. Rev. Cancer *7*, 733–736.

Götte, M., and Yip, G.W. (2006). Heparanase, hyaluronan, and CD44 in cancers: A breast carcinoma perspective. Cancer Res. *66*, 10233–10237.

Groupe d'Etude et de Traitement du Carcinome Hépatocellulaire. (1995). A comparison of lipiodol chemoembolization and conservative treatment for unresectable hepatocellular carcinoma. N. Engl. J. Med. *332*, 1256–1261.

Herrera, M.B., Bruno, S., Buttiglieri, S., Tetta, C., Gatti, S., Deregibus, M.C., Bussolati, B., and Camussi, G. (2006). Isolation and characterization of a stem cell population from adult human liver. Stem Cells *24*, 2840–2850.

Ho, J.W., Pang, R.W., Lau, C., Sun, C.K., Yu, W.C., Fan, S.T., and Poon, R.T. (2006). Significance of circulating endothelial progenitor cells in hepatocellular carcinoma. Hepatology *44*, 836–843.

Isabel, Z., Miri, B., Einav, H., Ella, B.L., Zamir, H., and Ran, O. (2006). Isolation, characterization and culture of Thy1-positive cells from fetal rat livers. World J. Gastroenterol. *12*, 3841–3847.

Jochum, W., Passegué, E., and Wagner, E.F. (2001). AP-1 in mouse development and tumorigenesis. Oncogene *20*, 2401–2412.

Karnoub, A.E., Dash, A.B., Vo, A.P., Sullivan, A., Brooks, M.W., Bell, G.W., Richardson, A.L., Polyak, K., Tubo, R., and Weinberg, R.A. (2007). Mesenchymal stem cells within tumour stroma promote breast cancer metastasis. Nature *449*, 557–563.

Kim, D.J., Chan, K.S., Sano, S., and Digiovanni, J. (2007). Signal transducer and activator of transcription 3 (Stat3) in epithelial carcinogenesis. Mol. Carcinog. *46*, 725–731.

Lara-Pezzi, E., Serrador, J.M., Montoya, M.C., Zamora, D., Yanez-Mo, M., Carretero, M., Furthmayr, H., Sanchez-Madrid, F., and Lopez-Cabrera, M. (2001). The hepatitis B virus X protein (HBx) induces a migratory phenotype in a CD44-dependent manner: Possible role of HBx in invasion and metastasis. Hepatology *33*, 1270–1281.

Lázaro, C.A., Croager, E.J., Mitchell, C., Campbell, J.S., Yu, C., Foraker, J., Rhim, J.A., Yeoh, G.C., and Fausto, N. (2003). Establishment, characterization, and long-term maintenance of cultures of human fetal hepatocytes. Hepatology *38*, 1095–1106.

Lee, H.C., Kim, M., and Wands, J.R. (2006). Wnt/Frizzled signaling in hepatocellular carcinoma. Front. Biosci. *11*, 1901–1915.

Li, C., Heidt, D.G., Dalerba, P., Burant, C.F., Zhang, L., Adsay, V., Wicha, M., Clarke, M.F., and Simeone, D.M. (2007). Identification of pancreatic cancer stem cells. Cancer Res. *67*, 1030–1037.

Liu, G., Yuan, X., Zeng, Z., Tunici, P., Ng, H., Abdulkadir, I.R., Lu, L., Irvin, D., Black, K.L., and Yu, J.S. (2006). Analysis of gene expression and chemoresistance of CD133+ cancer stem cells in glioblastoma. Mol. Cancer *5*, 67.

Llovet, J.M., Fuster, J., and Bruix, J. (1999). Intention-to-treat analysis of surgical treatment for early hepatocellular carcinoma: Resection versus transplantation. Hepatology *30*, 1434–1440.

Llovet, J.M., Burroughs, A., and Bruix, J. (2003). Hepatocellular carcinoma. Lancet *362*, 1907–1917.

Lo, C.M., Ngan, H., Tso, W.K., Liu, C.L., Lam, C.M., Poon, R.T., Fan, S.T., and Wong, J. (2002). Randomized controlled trial of transarterial lipiodol chemoembolization for unresectable hepatocellular carcinoma. Hepatology *35*, 1164–1171.

Ma, S., Chan, K.W., Hu, L., Lee, T.K., Wo, J.Y., Ng, I.O., Zheng, B.J., and Guan, X.Y. (2007). Identification and characterization of tumorigenic liver cancer stem/progenitor cells. Gastroenterology *132*, 2542–2556.

Mazzaferro, V., Regalia, E., Doci, R., Andreola, S., Pulvirenti, A., Bozzetti, F., Montalto, F., Ammatuna, M., Morabito, A., and Gennari, L. (1996). Liver transplantation for the treatment of small hepatocellular carcinomas in patients with cirrhosis. N. Engl. J. Med. *334*, 693–699.

McMahon, B.J. (2005). Epidemiology and natural history of hepatitis B. Semin. Liver Dis. *25* (*Suppl 1*), 3–8.

Minervini, M.I., Demetris, A.J., Lee, R.G., Carr, B.I., Madariaga, J., and Nalesnik, M.A. (1997). Utilization of hepatocyte-specific antibody in the immunocytochemical evaluation of liver tumors. Mod. Pathol. *10*, 686–692.

Nava, S., Westgren, M., Jaksch, M., Tibell, A., Broome, U., Ericzon, B.G., and Sumitran-Holgersson, S. (2005). Characterization of cells in the developing human liver. Differentiation *73*, 249–260.

O'Brien, C.A., Pollett, A., Gallinger, S., and Dick, J.E. (2007). A human colon cancer cell capable of initiating tumour growth in immunodeficient mice. Nature *445*, 106–110.

Pang, R.W., Lee, T.K., Man, K., Poon, R.T., Fan, S.T., Kwong, Y.L., and Tse, E. (2006). PIN1 expression contributes to hepatic carcinogenesis. J. Pathol. *210*, 19–25.

Paul, S.A., Simons, J.W., and Mabjeesh, N.J. (2004). HIF at the crossroads between ischemia and carcinogenesis. J. Cell. Physiol. *200*, 20–30.

Rege, T.A., and Hagood, J.S. (2006). Thy-1 as a regulator of cell-cell and cell-matrix interactions in axon regeneration, apoptosis, adhesion, migration, cancer, and fibrosis. FASEB J. *20*, 1045–1054.

Ricci-Vitiani, L., Lombardi, D.G., Pilozzi, E., Biffoni, M., Todaro, M., Peschle, C., and De Maria, R. (2007). Identification and expansion of human colon-cancer-initiating cells. Nature *445*, 111–115.

Seiki, M. (2003). Membrane-type 1 matrix metalloproteinase: A key enzyme for tumor invasion. Cancer Lett. *194*, 1–11.

Singh, S.K., Hawkins, C., Clarke, I.D., Squire, J.A., Bayani, J., Hide, T., Henkelman, R.M., Cusimano, M.D., and Dirks, P.B. (2004). Identification of human brain tumour initiating cells. Nature *432*, 396–401.

Suetsugu, A., Nagaki, M., Aoki, H., Motohashi, T., Kunisada, T., and Moriwaki, H. (2006). Characterization of CD133+ hepatocellular carcinoma cells as cancer stem/progenitor cells. Biochem. Biophys. Res. Commun. *351*, 820–824.

Tang, C., Ang, B.T., and Pervaiz, S. (2007). Cancer stem cell: Target for anticancer therapy. FASEB J. *21*, 3777–3785.

Tang, Z.Y., Ye, S.L., Liu, Y.K., Qin, L.X., Sun, H.C., Ye, Q.H., Wang, L., Zhou, J., Qiu, S.J., Li, Y., et al. (2004). A decade's studies on metastasis of hepatocellular carcinoma. J. Cancer Res. Clin. Oncol. *130*, 187–196.

Tian, J., Tang, Z.Y., Ye, S.L., Liu, Y.K., Lin, Z.Y., Chen, J., and Xue, Q. (1999). New human hepatocellular carcinoma (HCC) cell line with highly metastatic potential (MHCC97) and its expressions of the factors associated with metastasis. Br. J. Cancer *81*, 814–821.

Yang, Z.F., Poon, R.T., To, J., Ho, D.W., and Fan, S.T. (2004a). The potential role of hypoxia inducible factor 1alpha in tumor progression after hypoxia and chemotherapy in hepatocellular carcinoma. Cancer Res. *64*, 5496–5503.

Yang, Z.F., Poon, R.T., Luo, Y., Cheung, C.K., Ho, D.W., Lo, C.M., and Fan, S.T. (2004b). Upregulation of vascular endothelial growth factor (VEGF) in small-for-size liver grafts enhances macrophage activities through VEGF receptor 2 (Flk-1)-dependent pathway. J. Immunol. *173*, 2507–2515.

Yang, Z.F., Ho, D.W., Lam, C.T., Luk, J.M., Lum, C.T., Yu, W.C., Poon, R.T., and Fan, S.T. (2005). Identification of brain-derived neurotrophic factor (BDNF) as a novel functional protein in hepatocellular carcinoma. Cancer Res. *65*, 219–225.

Yin, S., Li, J., Hu, C., Chen, X., Yao, M., Yan, M., Jiang, G., Ge, C., Xie, H., Wan, D., et al. (2007). CD133 positive hepatocellular carcinoma cells possess high capacity for tumorigenicity. Int. J. Cancer *120*, 1436–1442.